

Electric Field Manipulation of Charged Copolymer Worm Micelles[†]

Kandaswamy Vijayan, Yan Geng, and Dennis Discher*

Graduate Group in Physics, Chemical & Biomolecular Engineering, and The Laboratory for Research on the Structure of Matter, University of Pennsylvania, Philadelphia, Pennsylvania 19104

Received: September 16, 2005; In Final Form: November 4, 2005

Manipulation of diblock copolymer worm micelles by external electric fields is visualized by fluorescence microscopy in dilute, aqueous solution. Hydrodynamic coupling of the poly(acrylic acid)–(1,4)-polybutadiene (PAA–PBD) worm motion to the electric field and the effective stiffening of the worms in an oscillating electric field are demonstrated. A brief discussion on using this technique to estimate the rheological properties of wormlike micelles is presented.

Introduction

Manipulation of suspended colloids by electric fields serves many purposes, from separation of biomolecular colloids such as DNA¹ to directed assembly of nanowires from polymer-based or metallic nanoparticles.² Block copolymer amphiphiles can also assemble into highly stable colloids, in simulation³ as well as in experiment.^{4,5} Morphologies include micrometer-long worm micelles⁶ as well as branched networks⁷ and string-of-pearl shapes⁸ that raise fundamental questions about responses in electric fields. While *E*-fields have been applied to align bulk cylinder phases of block copolymers in creating and controlling nanopatterns,⁹ it is not clear to what extent *E*-fields disrupt individual, self-assembled structures. Electroporation of related copolymer-based vesicles, or polymersomes, has already demonstrated poration or rupture under sub-millisecond pulses of less than 9 V.¹⁰ Here, we show that polymer-based worm micelles are electrostable and also alignable, under nominally similar conditions.

Surfactant wormlike micelles have been studied in shear fields in order to understand both their complex rheology¹¹ and transport behavior. Their flow through nanoporous gels has been visualized using fluorescence microscopy of dye-labeled worms to show that they can reptate through gels where vesicles are filtered out.¹² The block copolymer constituents specify worm micelle properties such as diameter, which increases with molecular weight, and flexibility or persistence length, which increases with diameter according to d^3 -scaling of a fluid cylinder.⁶ While neutral diblocks of poly(ethylene oxide)–polybutadiene (PEO–PBD) have contributed many such insights to date, surface charge density can also be controlled. Worm micelles, micrometers in length, made from poly(acrylic acid)–(1,4)-polybutadiene (PAA–PBD) diblocks were recently described as fluid and flexible in solution in addition to being stable depending on pH and salt conditions.¹³ For neutral and charged worm micelles, fluorescence microscopy has been the primary tool to quantify flexibility and dynamic processes ranging from free relaxation¹⁴ to microphase transitions into spheres.^{13,15} Visualization of worm dynamics in oscillating

electric fields is used here to quantify the voltage scaling of electrophoresis and a quasi-resonant stretching of charged worms.

We use a simple experimental setup with an external oscillating electric field to manipulate cylindrical micelles that contain neutral and/or charged polymers. Experiments were performed at pH 6.5, where PAA is negatively charged and where worm micelles are the favored morphology. Briefly, we find that the velocities of the worms are independent of their length but linearly dependent on voltage, consistent with a simple electrophoretic mobility. We also observe a suppression of thermal fluctuations of the worms in an intermediate range of driving frequencies between 0.1 and 100 Hz, which makes the effective stiffness response resemble the resonance peak of a forced harmonic oscillator with damping. The resonance frequency corresponds to the natural time scale of fluctuations in the worm backbone.

Experimental Details

Materials. Details of diblock copolymers AB2 (PAA₇₅–PBD₁₀₃, M_n 11.05 kg/mol) and OB18 (PEO₈₀–PBD₁₂₅, M_n 10.4 kg/mol) are provided elsewhere.^{6,13} Chloroform, glass slides, and coverslips were purchased from Fisher. The hydrophobic dye PKH26, HCl, and NaOH were purchased from Sigma-Aldrich. Additionally, the Circuit Writer, precision conducting ink dispenser (CAIG Labs, Inc.), was purchased from Radio Shack.

Preparation of Worm Micelles. Worm micelles were prepared by the film-rehydration method (details published elsewhere).¹⁴ Briefly, 10 μ L of copolymer stock solution was put into a clean glass vial and the chloroform evaporated under nitrogen. The polymer film deposited was further dried by placing it in a vacuum chamber for 6 h. Worm micelles were formed upon rehydrating the thin film with 1 mL of aqueous solution of the desired pH (by addition of HCl and NaOH).

Fluorescence Microscopy and Electric Field. The cores of the micelles were labeled by 1 μ L of hydrophobic fluorophore PKH26 to enable visualization under fluorescence microscopy. The experimental chamber was prepared by placing 5–10 μ L of worm solution between a glass slide and specially sized 1.25 cm \times 2.5 cm rectangular coverslip. The long edges were sealed by a liberal coating of conducting ink, and vacuum grease was used to seal the other two edges to make a leakproof chamber.

[†] Part of the special issue “Michael L. Klein Festschrift”.

* To whom correspondence should be addressed. E-mail: discher@seas.upenn.edu.

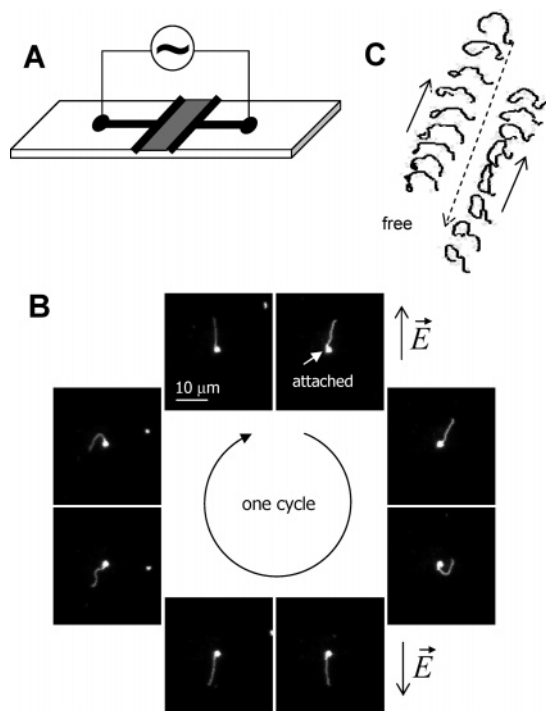


Figure 1. Schematic of the electromanipulation chamber. (A) A dilute solution of worm micelles is placed in a chamber formed between a slide and coverslip ($2.5\text{ cm} \times 1.25\text{ cm}$). Two edges are sealed using a quick drying conducting-polymer-based ink (the electrodes), and the other two, with vacuum grease. Electrodes are connected to a signal generator using alligator clips. (B) Fluorescence snapshots of a surface-attached worm moving back and forth in a field. (C) Trace of a $12\text{ }\mu\text{m}$ worm moving back and forth for 1.5 cycles in a 0.1 Hz, 9 V electric field. The motion in the forward direction only is shown. The prominence of the \cap shaped configuration can be seen.

Electrodes, leading from the edge of the coverslip, were drawn onto the glass slide and alligator clips were clamped to the ends to enable electrical contact with a signal generator (Good Will Instruments Co. Ltd., Taipei, model GFG-8020G). The technical challenge of applying an electric field in a few micrometer thick chamber was thus met by using conducting ink ($5\text{ }\mu\text{m}$ silver particles in a matrix of conducting polymers), which acts as both sealant and electrodes spaced at $\sim 1.25\text{ cm}$. This experimental design can be applied to many similar microsystems. Sine, pulse, and sawtooth signals at different frequencies and amplitudes were used to manipulate the worm motion. Solutions (0.1 mg/mL) of OB18 and AB2 worm micelles prepared as above were diluted 5-fold on the microscope slide to obtain images of well-separated worm micelles.

Result and Discussion

Charged versus Uncharged Worms. Mean contour lengths of both neutral OB18 worms and charged AB2 worms ranged from 10 to $20\text{ }\mu\text{m}$ and were therefore easily visualized by optical microscopy (Figure 1B). Occasionally, the worms attached to the surface, but most were freely diffusing, undergoing Brownian motion. To set the worms in motion (and test electrostaticity), the signal generator was set to 9 V (peak–peak) and 0.1 Hz. A sawtooth signal was applied and provided a smooth transition between the forward and backward movements of the worms, with a maximum distance traversed that was fairly constant after many periods. Square wave and sine wave signals caused the worms to stall briefly during the transition from forward to backward motion (less so for the sine wave), leading to a drift in the displacement amplitude. A sawtooth pulse was

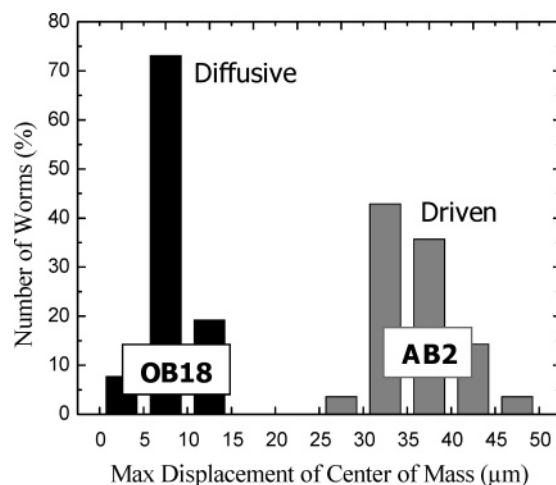


Figure 2. Motion of neutral and charged worms in an oscillating electric field. (A) The average contour length of both the OB18 and AB2 worms is $\sim 15\text{ }\mu\text{m}$. When an electric field of 9 V and 0.1 Hz is applied, both worms are observed to exhibit oscillatory motion, but the charged AB2 worms move severalfold further than OB18 worms whose motion is considered largely diffusive. Distributions in displacements are most likely due to slight variations in the field strength due to uneven electrodes as well as weak hydrodynamic variations.

therefore used in all of the experiments unless otherwise indicated. As shown in Figure 1B,C and plotted in Figure 2, not only do the charged AB2 worms stay intact but their centers of mass are driven on average 30–40 μm during half a cycle (by 9 V), whereas the uncharged OB18 micelles moved a mere 5–10 μm in a similar interval of imaging. This distance for the neutral worms is in the range of their contour lengths and can therefore be considered largely diffusive motion.

Displacement of Charged Worms as a Function of Contour Length. The distance between the turnaround points of the worm motion was measured as a function of worm contour length. The 0.1 Hz electric field was set to 9 V or more, and it was observed that an increased voltage causes an overall increase in the displacement of the worms. However, for a fixed voltage, the worms traversed similar distances irrespective of their contour lengths (Figure 3A). While longer worms might be expected to move further (faster) in the field because they carry more charge in proportion to their length, the fluid-imposed drag also scales with length in the Rouse limit.¹⁶ The same observations are made for DNA electrophoresis, motivating the use of media (e.g., agarose gels) that foster nonlinear drag phenomena such as entanglements and reptation.¹⁷ Although the worm displacements appear independent of length, the maximum displacements increase linearly with increasing voltage (Figure 3B).

The intercept of $\sim 10\text{ }\mu\text{m}$ is again largely indicative of chain diffusion (as with neutral worms, Figure 2). However, the slope ($\mu\text{m/V}$) yields an electrophoretic mobility, μ , related to the effective charge density scaled by the hydrodynamic drag per length (for Rouse chains). This mobility is calculated from the product of displacement and frequency divided by the electric field as the voltage between the spaced electrodes: $\mu \approx (2.5\text{ }\mu\text{m/V}) \times (0.1\text{ s}^{-1}) \times (1.25\text{ cm}) = 3.1 \times 10^{-5}\text{ cm}^2\text{ V}^{-1}\text{ s}^{-1}$. This is 10-fold lower than the μ reported for small DNA and RNA segments.¹⁸

Effective Stiffness of Worm Micelle as a Function of Frequency. The stiffness of worm micelles in solution, in the absence of a field, is revealed in the thermal fluctuations of its contour. This is characterized by a persistence length, l_p , obtained most simply from the relation $\langle R^2 \rangle = 2l_p^2[L/l_p - 1 +$

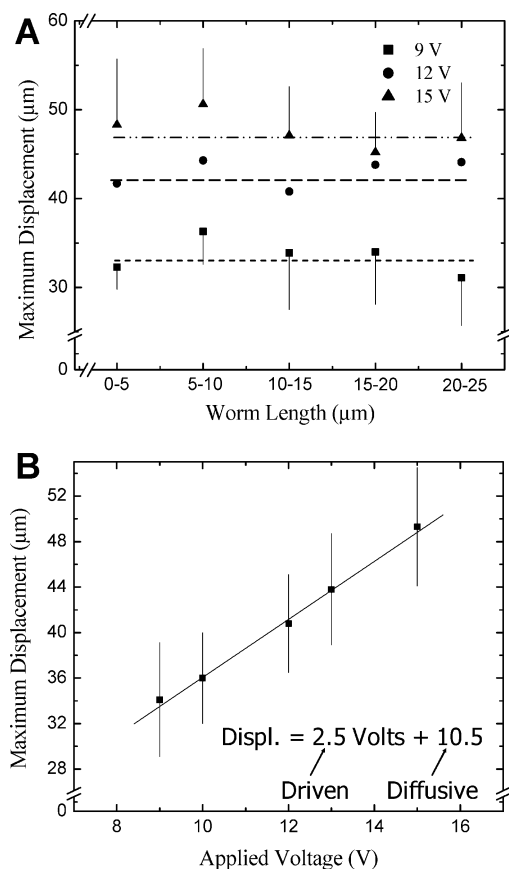


Figure 3. Charged worm dynamics as a function of voltage. (A) Different voltages at a frequency of 0.1 Hz are applied across a sample of AB2 worms, and the maximum displacement of the center of mass in half a cycle is found to be independent of the contour length. (B) In the range of voltages from 9 to 15 V, the maximum displacement of AB2 worms depends linearly on the field strength (at 0.1 Hz). Electrophoretic mobility can be calculated from the slope of the curve, as described in the text.

$\exp(-L/l_p)$, where L is the contour length and R is the end-to-end distance of the worm.¹⁴ In the absence of an electric field, the persistence length of the charged AB2 worm micelles averages 3 μm, which is in good agreement with the first reports on these worm micelles.¹³ However, when AB2 worm micelles are subjected to an oscillating electric field at low frequency (0.1 Hz), the effective l_p decreases to 2 μm. The stiffness increases with frequency to reach a maximum of 5 μm at around 3 Hz, where the worms appear to be fully stretched out and their fluctuation decreases dramatically (Figure 4). As the frequency is further increased, the stiffness of AB2 worms gradually decreases to a value near the low frequency value.

While no significant correlation was observed between the stiffness changes and the strength of the field in the range tried (9–15 V), the rapid back-and-forth movement of a worm in a fluid medium clearly suppresses the Brownian dynamics of the worm. The field influences the normal modes of the worms by imposing a larger force on the body of the worms compared to the ends during field reversal. The body of the worms is observed to be pushed faster than the ends, resulting in U shaped configurations at the turnaround points. As the oscillating frequency is increased (up to 5 Hz), the frequency of the turnarounds increases and the time interval between U and \cap shaped configurations decreases, resulting in a gradual flattening out of the worm backbone and an increased stiffness. At frequencies greater than 5 Hz, the coupling between the fluid motion and worm dynamics changes in character. The strong

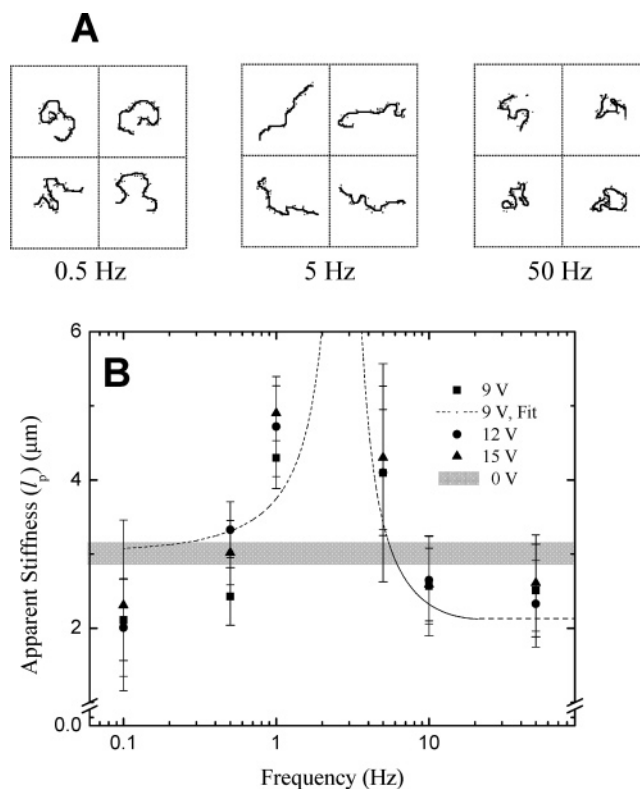


Figure 4. Charged worm dynamics as a function of driving frequency. (A) Backbone traces of four random fluorescent snapshots of a worm moving in different frequencies of a 9 V sawtooth with the field oriented vertically, per Figure 1B. The images have been slightly moved from their original positions to show the different configurations more clearly. All worms are around 20 μm in contour length. Stiffening of the worms can be clearly observed at 5 Hz. (B) The effective stiffness of the worms, l_p , is calculated per the text, and the 9 V stiffness curve has been fitted to a forced harmonic oscillator amplitude, $y = y_0 + A/\sqrt{((\omega_0^2 - \omega^2)^2 + (\beta\omega)^2)}$, where β is the damping coefficient and A , y_0 , and ω_0 —the resonance frequency—are fitting parameters. The stiffness vs frequency curve is similar across three different voltages in a small range.

coupling with the back-and-forth motion of the field is lost, and the worms explore more of their natural configurations, albeit in a sporadic manner. The rapid jiggling of the worms causes them to “freeze” momentarily in configurations until a threshold fluctuation passes through the backbone that causes it to move into another configuration. This indicates coupling of the field with higher relaxation modes of fluctuations. Worms do not seem to favor stretched out configurations under high oscillation frequencies, as reflected in a decreasing stiffness compared to the case of zero field.

The coupling of the electric field to the worm motion can be likened to a driven, damped harmonic oscillator with a resonance frequency that corresponds to the natural relaxation time scale of the worm fluctuation in the field. Fitting the effective stiffness versus frequency to the model amplitude of a driven, damped harmonic oscillator leads to a resonance frequency of ~ 3 Hz and an amplitude of ~ 10 – 15 μm. While the amplitude approximates the contour length, L , the resonance time scale of $\tau \sim 0.3$ s can be interpreted as the relaxation time of the backbone for AB2 worms in a field. The only other measurements of relaxation times for micrometer-long block copolymer micelles are for smaller diameter, more flexible, neutral worms in thermal equilibrium where $l_p \sim 0.5$ and $\tau \sim 3$ s.¹⁴ One expects from classic oscillator theory that $\tau \sim 1/l_p^{1/2}$, and thus, lower resonance frequencies in the range of ~ 1 s are certainly expected from prior work.

Conclusion

We present a simple experimental setup for manipulating and studying the dynamics of cylindrical diblock copolymer worm micelles. A few basic proof-of-concept experiments are presented to assess the mobility and relaxation time scales of flexible filaments. Applications might include *E*-field driven carriers or microfluidic stirring with tethered micelles that coordinate flagellar motions. While the current study was restricted to low electric fields, this can be pushed further to attempt breakage of these remarkably stable worm micelles.

Acknowledgment. Funding for this project was provided by NSF-MRSEC.

References and Notes

- (1) Viovy, J.-L. *Rev. Mod. Phys.* **2000**, 72, 813.
- (2) Velev, O. D.; Lenhoff, A. M.; Kaler, E. W. *Science* **2000**, 287, 2240.
- (3) Srinivas, G.; Discher, D. E.; Klein, M. L. *Nat. Mater.* **2004**, 3, 638.
- (4) Antonietti, M.; Forster, S. *Adv. Mater.* **2003**, 15, 1323.
- (5) Discher, D. E.; Eisenberg, A. *Science* **2002**, 297, 967.
- (6) Dalhaimer, P.; Bermudez, H.; Discher, D. E. *J. Polym. Sci., Part B: Polym. Phys.* **2004**, 42, 168–176.
- (7) Jain, S.; Bates, F. S. *Science* **2003**, 300, 460.
- (8) Discher, D. E.; Kamien, R. D. *Nature* **2004**, 430, 519.
- (9) Thurn-Albrecht, T.; et al. *Science* **2000**, 290, 2126.
- (10) Aranda-Espinoza, H.; Bermudez, H.; Bates, F. S.; Discher, D. E. *Phys. Rev. Lett.* **2001**, 87, 208.
- (11) Walker, L. M. *Curr. Opin. Colloid Interface Sci.* **2001**, 6, 451.
- (12) Kim, Y.-H.; Pajerowski, D.; Christian, D. A.; Discher, D. E. *Nanotechnology* **2005**, 16, 484.
- (13) Geng, Y.; Ahmed, F.; Bhasin, N.; Discher, D. E. *J. Phys. Chem. B* **2005**, 109, 3772.
- (14) Dalhaimer, P.; Bates, F. S.; Discher, D. E. *Macromolecules* **2003**, 36, 6873.
- (15) Geng, Y.; Discher, D. E. *J. Am. Chem. Soc.* **2005**, 127, 12780.
- (16) Strobl, G. R. *The Physics of Polymers*, 2nd ed.; Springer: New York, 1997; Chapter 6.
- (17) Bloomfield, V. A. *Annu. Rev. Phys. Chem.* **1977**, 28, 233.
- (18) Hummer, G.; Yeh, I.-C. *Biophys. J.* **2004**, 86, 681.